Letter

Attractive Su-Schrieffer-Heeger-Hubbard model on a square lattice away from half-filling

Bo Xing [1,*] Chunhan Feng,[2,3] Richard Scalettar,[3] G. George Batrouni,[4,5,6] and Dario Poletti[1,7,4,8]

[1]*Science, Mathematics and Technology Cluster, Singapore University of Technology and Design,*
8 Somapah Road, Singapore 487372, Singapore
[2]*Center for Computational Quantum Physics, Flatiron Institute, 162 5th Avenue, New York, New York 10010, USA*
[3]*Department of Physics, University of California, Davis, California 95616, USA*
[4]*Centre for Quantum Technologies, National University of Singapore, 2 Science Drive 3, Singapore 117542, Singapore*
[5]*Department of Physics, National University of Singapore, 2 Science Drive 3, Singapore 117542, Singapore*
[6]*Université Côte d'Azur, CNRS, Institut de Physique de Nice (INPHYNI), 06000 Nice, France*
[7]*EPD Pillar, Singapore University of Technology and Design, 8 Somapah Road, Singapore 487372, Singapore*
[8]*MajuLab, CNRS-UNS-NUS-NTU International Joint Research Unit, UMI 3654, Singapore*

The Su-Schrieffer-Heeger (SSH) model, with bond phonons modulating electron tunneling, is a paradigmatic electron-phonon model that hosts an antiferromagnetic order to bond order transition at half-filling. In the presence of a repulsive Hubbard interaction, the antiferromagnetic phase is enhanced, but the phase transition remains first order. Here, we explore the physics of the SSH model with an *attractive* Hubbard interaction, which hosts an interesting interplay among charge order, *s*-wave pairing, and bond order. Using the numerically exact determinant quantum Monte Carlo method, we show that both charge order, present at weak electron-phonon coupling, and bond order, at large coupling, give way to *s*-wave pairing when the system is doped. Furthermore, we demonstrate that the SSH electron-phonon interaction competes with the attractive Hubbard interaction and reduces the *s*-wave pairing correlation.

Introduction. Electron-electron and electron-phonon correlations are two fundamental interactions in condensed matter quantum many-body systems. The basic qualitative features of the electron-electron interaction are famously studied in the Hubbard model [1–5], which, depending on the interaction's magnitude and doping, can exhibit metallic phases, long-range spin/charge patterns, and superconducting pairing [6–10]. Similarly, the phenomena induced by the electron-phonon interaction are often studied in the Holstein [11] and Su-Schrieffer-Heeger (SSH) [12] models. The former considers site phonon vibrations that influence the on-site chemical potential and can result in charge density wave (CDW) and *s*-wave pairing [13–27]. The latter considers bond phonon vibrations that modulate nearest-neighbor tunneling and give rise to antiferromagnetic order and bond order wave (BOW) [28–41].

The interplay between the electron-electron and the electron-phonon interactions has attracted a lot of attention. Extensive studies on the repulsive Hubbard-Holstein model at half-filling have shown that magnetic and charge order dominates in the strong electron-electron and electron-phonon interaction regimes, respectively [42–46]. Where the electron-electron and electron-phonon interactions are comparable, numerical simulations reveal a metal or superconducting pairing phase [47–50]. Away from half-filling, Monte Carlo simulations are severely undermined by the sign problem

[51–55], and numerical evidence predicts either superconducting pairing or stripe order [48,56].

The combined effects of SSH phonons with Hubbard interactions have only been more recently investigated. The repulsive SSH-Hubbard (SSHH) model on a square lattice features a direct first-order transition between antiferromagnetic order and BOW at half-filling [57,58]. The repulsive SSHH model also suffers from a sign problem away from half-filling. Nonetheless, a density matrix renormalization group study on narrow two-dimensional (2D) cylinders and a functional renormalization group study of square lattices have shown evidence of superconducting pairings around 1/8 doping [59,60].

In the above studies, the on-site electron-electron interaction was taken to be repulsive. However, a similar, and potentially rich, phenomenology is expected at the interplay between the electron-phonon interaction and *attractive* on-site electron-electron interactions. In particular, the attractive Hubbard model exhibits a competition between charge order and *s*-wave pairing [61–64], with bond order due to SSH phonons. Importantly, the attractive SSHH model does not suffer from the sign problem. This makes it a rare electron-electron and electron-phonon model that can be studied exactly at all fillings and low temperatures.

In this Letter, we present a study of the single-orbital square lattice attractive SSHH model with periodic boundary conditions. We consider the full phonon dynamics and focus on the phase transitions away from half-filling. Due to the absence of the sign problem, we can simulate systems of up to 12×12 spatial sites at low temperatures using the

determinant quantum Monte Carlo (DQMC) method [13,65–68]. First, we show the effects of an attractive interaction in the half-filled BOW ground state. In addition, we analyze the effect of temperature and phonon frequency on the ground state phase transitions. At half-filling, the system presents either a charge density wave or bond order depending on the magnitude of the electron-phonon interactions. Larger attractive interactions reduce the bond order. Away from half-filling the system abruptly goes into an *s*-wave pairing ordered phase independent of the magnitude of the electron-phonon interaction.

Model and method. The attractive SSHH Hamiltonian is

$$\hat{\mathcal{H}} = -t \sum_{\langle i,j \rangle, \sigma} (1 - \lambda \hat{X}_{ij})(\hat{c}_{i\sigma}^{\dagger}\hat{c}_{j\sigma} + \text{H.c.}) - \mu \sum_{i,\sigma} \hat{n}_{i\sigma}$$

$$+ U \sum_{i} \left(\hat{n}_{i\uparrow} - \frac{1}{2} \right) \left(\hat{n}_{i\downarrow} - \frac{1}{2} \right)$$

$$+ \sum_{\langle i,j \rangle} \left(\frac{1}{2M} \hat{P}_{ij}^2 + \frac{M}{2} \omega_0^2 \hat{X}_{ij}^2 \right), \quad (1)$$

where $\hat{c}_{i\sigma}$ ($\hat{c}_{i\sigma}^{\dagger}$) destroys (creates) an electron of spin $\sigma = \uparrow, \downarrow$ on site i, U is the strength of the electron-electron interaction, $\hat{n}_{i\sigma} = \hat{c}_{i\sigma}^{\dagger}\hat{c}_{i\sigma}$ is the number operator, M is the phonon mass, and ω_0 the phonon frequency. $\hat{X}_{ij}$ and $\hat{P}_{ij}$ are the canonically conjugate phonon displacement and momentum. The dimensionless electron-phonon coupling strength is $g = \lambda/\sqrt{2M\omega_0/\hbar}$. When $U < 0$, the Hubbard interaction is attractive. The chemical potential μ controls the density of the system. The system is at half-filling, $\langle n \rangle = \sum_i \langle \hat{n}_{i\uparrow} + \hat{n}_{i\downarrow} \rangle / N = 1$, for $\mu = 0$. In an ordered phase, a gap can open such that the system leaves half-filling only beyond a finite critical μ_c. The value of μ_c depends on the other system parameters. Here, we work in units where $\hbar = M = t = k_B = 1$ (k_B is the Boltzmann constant).

The attractive SSHH model does not suffer from the sign problem because both the SSH phonons, the chemical potential, and the Hubbard-Stratonovich [69–73] field couple to the spin-up and spin-down electrons identically. Consequently, the determinants that arise from integrating the fermionic degrees of freedom are identical for the two spin species, and the configurational weight is a perfect square. We work with inverse temperature $\beta = L_\tau \Delta\tau = 16t$, $21t$, $24t$, where $L_\tau = 300$ is the number of imaginary time steps. Even for the largest value of $\Delta\tau = 0.08t$, the estimate of the Trotter error is of the same order as the statistical error bars in the structure factors. In addition, to elucidate finite-size effects, we compare three $L \times L$ systems with $L = 8, 10, 12$.

To characterize the underlying ground state phases in different parameter regimes, we calculate the CDW correlations and structure factors, $C_{\text{CDW}}(i, j) = \langle (\hat{n}_{i,\uparrow} + \hat{n}_{i,\downarrow})(\hat{n}_{j,\uparrow} + \hat{n}_{j,\downarrow}) \rangle$ and their Fourier transform $S_{\text{CDW}}(q) = \frac{1}{N} \sum_{i,j} e^{iq(i-j)} C_{\text{CDW}}(i, j)$, and the BOW correlations and structure factors, $C_{\text{BOW}}(i, j) = \sum_{\sigma} \langle \hat{c}_{i,\sigma}^{\dagger} \hat{c}_{i+\hat{x}(\hat{y}),\sigma} \hat{c}_{j,\sigma}^{\dagger} \hat{c}_{j+\hat{x}(\hat{y}),\sigma} \rangle$ and its Fourier transform $S_{\text{BOW}}(q) = \frac{1}{N} \sum_{i,j} e^{iq(i-j)} C_{\text{BOW}}(i, j)$, respectively. In the rest of this Letter, we take $q = (\pi, \pi)$ as the default whenever $S_{\text{BOW/CDW}}$ is mentioned. The $S_{\text{BOW/CDW}}$ for all $q \neq (\pi, \pi)$ were measured but are negligible. The various wave pairing correlations are

characterized by $\mathcal{P}(i, j) = \langle \hat{\Delta}(j) \hat{\Delta}^{\dagger}(i) \rangle$ [74]. For the case of *s*-wave pairing, $\hat{\Delta}^{\dagger}(i) = \hat{c}_{i,\uparrow}^{\dagger} \hat{c}_{i,\downarrow}^{\dagger}$. The average density $\langle n \rangle$ is also useful in giving insight into the properties of the phases.

Results. Regardless of the sign of U, on a bipartite lattice, performing a (staggered) particle-hole transformation on both electron species changes the sign of the chemical potential while leaving the Hamiltonian and the spin, charge, and pair correlations invariant. As a consequence, the phase diagram is symmetrical under reflection about the point $\langle n \rangle = 1$. Furthermore, on a bipartite lattice precisely at $\langle n \rangle = 1$ ($\mu = 0$), the repulsive SSHH model can be transformed into the attractive SSHH model by performing a *partial* particle-hole transformation on one of the two electron species. Therefore, the phase diagram of the attractive model can be inferred from that of the repulsive model at $\langle n \rangle = 1$. Importantly, via the partial particle-hole transformation the magnetic order in the repulsive SSHH model is transformed into *s*-wave pairing correlations and charge order in the attractive SSHH model at half-filling.

Away from half-filling, the repulsive SSHH model no longer directly maps to the attractive SSHH model. We first investigate the effects of the electron-electron coupling U in a situation of large electron-phonon coupling, $g = 1.2$, where the system is firmly in the SSH BOW phase at half-filling. We will then consider the effect of the electron-phonon coupling g on the degenerate CDW/*s*-wave pairing phase which arises when U is the dominant energy scale.

In Fig. 1, we fix the electron-phonon coupling $g = 1.2$, phonon frequency $\omega_0 = 1.0t$, vary the chemical potential μ, and investigate the effects of the electron-electron coupling U. At $\mu = 0$, the ground state is a gapped $q = (\pi, \pi)$ BOW in either the x or y direction for all $U/t = 0, -4, -8$ [Fig. 1(a)]. When $|\mu|$ is lower than the critical $|\mu_c|$, the average density is pinned at $\langle n \rangle = 1$ and the system stays in a gapped (π, π) BOW phase. The CDW structure factor S_{CDW} and *s*-wave pairing correlation $\mathcal{P}_s$ are negligible when compared to the BOW structure factor S_{BOW}. At finite U and $\mu = \mu_c$, there is a noticeable increase of *s*-wave pairing $\mathcal{P}_s$ [Fig. 1(c)] [75]. In addition, $\langle n \rangle$ starts to decrease and S_{BOW} falls discontinuously within a narrow range of $\Delta\mu$ in Fig. 1(d). This suggests a first-order transition from the BOW phase to *s*-wave pairing in the attractive SSHH model. As U increases in magnitude, μ_c shifts towards $\mu = 0$ and *s*-wave pairing correlations increase. Interestingly, the BOW structure factor is also slightly enhanced in the presence of U before the transition. There is a qualitative change in S_{CDW} at μ_c as shown in Fig. 1(b). For this (large) value of electron-phonon coupling, $g = 1.2$, there is no CDW order at any filling including $\langle n \rangle = 1$.

Next, we show that the inverse temperature β we use is large enough to capture the ground state properties and study the effect of the phonon frequency ω_0 on the phase transition. In Fig. 2, we fix $U = -8t$, $g = 1.2$, and show structure factor data for different β [Figs. 2(a) and 2(c)] and ω_0 [Figs. 2(b) and 2(d)]. For Figs. 2(a) and 2(c), $\omega_0 = 1.0t$ and β is varied. There are no qualitative and only minor quantitative changes in the structure factors and μ_c as βt increases from 16 to 24. The transition between BOW and *s*-wave pairing remains first order and μ_c increases very slightly. For Figs. 2(b) and 2(d), $\beta = 16/t$ and ω_0 is varied. At $\omega_0 = 0.7$, we see a similar rapid decrease in S_{BOW}. The increase in $\mathcal{P}_s$ is much less apparent.
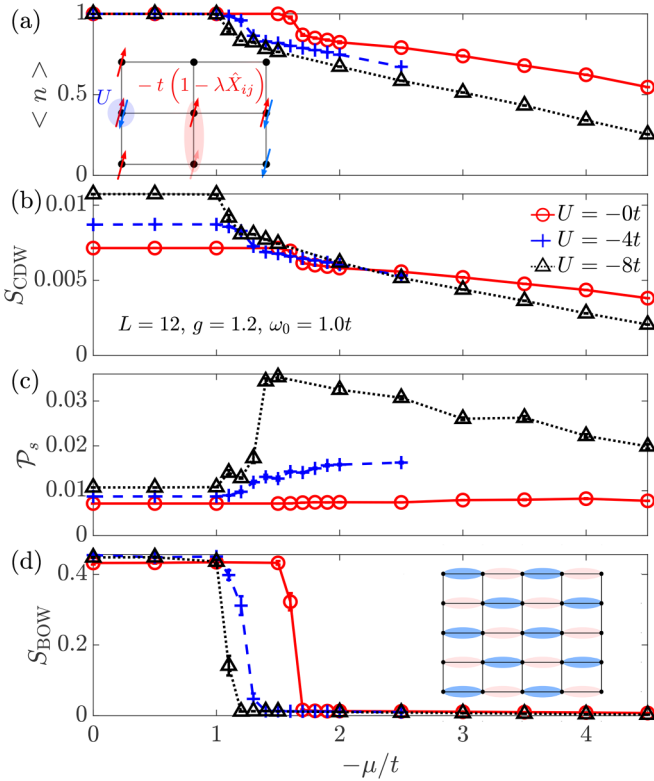
FIG. 1. (a) Average density $\langle n \rangle$, (b) CDW structure factor S_{CDW}, (c) s-wave pairing correlation $\mathcal{P}_s$, and (d) BOW structure factor S_{BOW} as functions of chemical potential μ. Inset of (a): Graphical representation of the electron-electron and electron-phonon interactions. Inset of (d): Graphical representation of the $q = (\pi, \pi)$ BOW. Different bond colors emphasize the alternation in bond lengths. In all panels, $L = 12$, electron-phonon coupling $g = 1.2$, and phonon frequency $\omega_0 = 1.0t$.

However, we cannot rule out the existence of a small nonzero pairing order at small ω_0. Numerical evidence of s-wave pairing has always been difficult in electron-phonon models, especially at lower ω_0. In the Holstein model, s-wave pairing is known to increase with ω_0 [22,48,76]. At low ω_0, the order parameter is likely to be small, if it exists. The situation is similar in the attractive SSHH model. At higher ω_0, the lattice responds more quickly to electronic hopping, and the electron-phonon fluctuation is suppressed. As a result, $\mathcal{P}_s$ is higher. The critical μ_c needed to leave half-filling decreases and so does S_{BOW} within the BOW phase. For all ω_0 that support BOW at half-filling, the BOW phase transitions directly to s-wave pairing.

In the above analysis, we investigated the effects of the electron-electron coupling U on the SSH BOW. Next, we study the effects of the electron-phonon coupling g on the properties of the attractive Hubbard model, specifically, how g and doping affect the degenerate CDW/s-wave pairing phase in the ground state at half-filling, and the superconducting phase (with a finite-T Kosterlitz-Thouless transition [77]).

In Fig. 3, we plot the average density $\langle n \rangle$ [Fig. 3(a)], CDW structure factor S_{CDW} [Fig. 3(b)], s-wave pairing correlation $\mathcal{P}_s$ [Fig. 3(c)], and BOW structure factor S_{BOW} [Fig. 3(d)] versus the chemical potential for $L = 12$, $U = -8t$, $\omega_0 = 1.0t$.
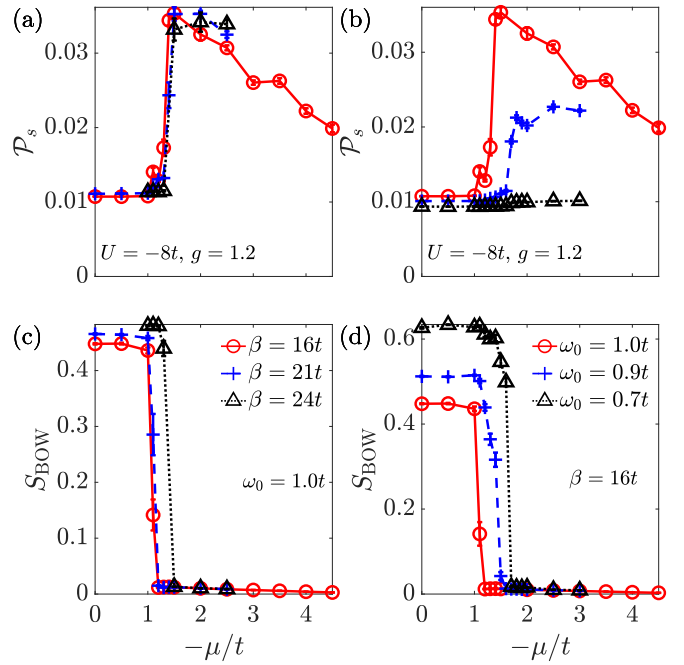

FIG. 2. (a), (b) s-wave pairing correlation $\mathcal{P}_s$ and (c), (d) BOW structure factor S_{BPW} against chemical potential μ. For all results, $L = 12$ and electron-phonon coupling $g = 1.2$. (a), (c) β is varied and ω_0 is fixed. (b), (d) ω_0 is varied and $\beta = 16$.
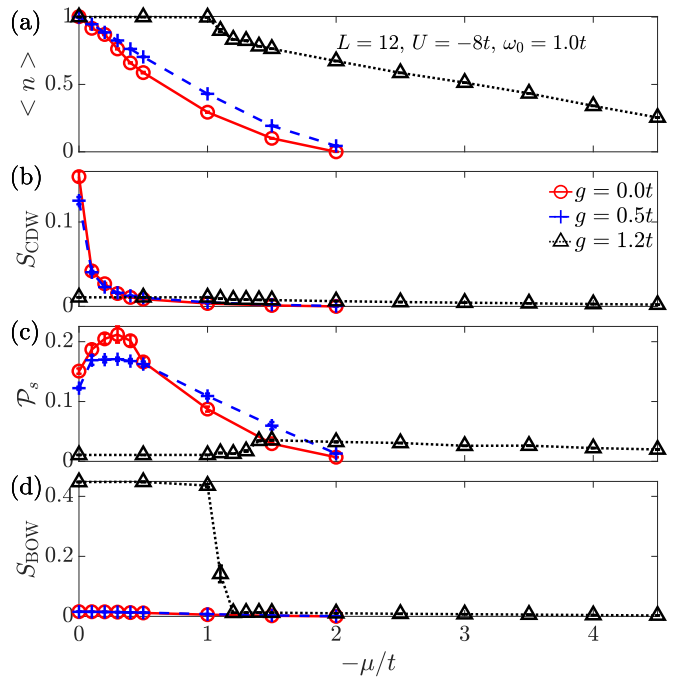

FIG. 3. (a) Average density $\langle n \rangle$, (b) CDW structure factor S_{CDW}, (c) s-wave pairing correlation $\mathcal{P}_s$, and (d) BOW structure factor S_{BOW} against chemical potential μ. For all results, system size $L = 12$, electron-electron coupling $U = -8t$, and phonon frequency $\omega_0 = 1.0t$. At $g = 0.0$, the system is described by the attractive Hubbard model.
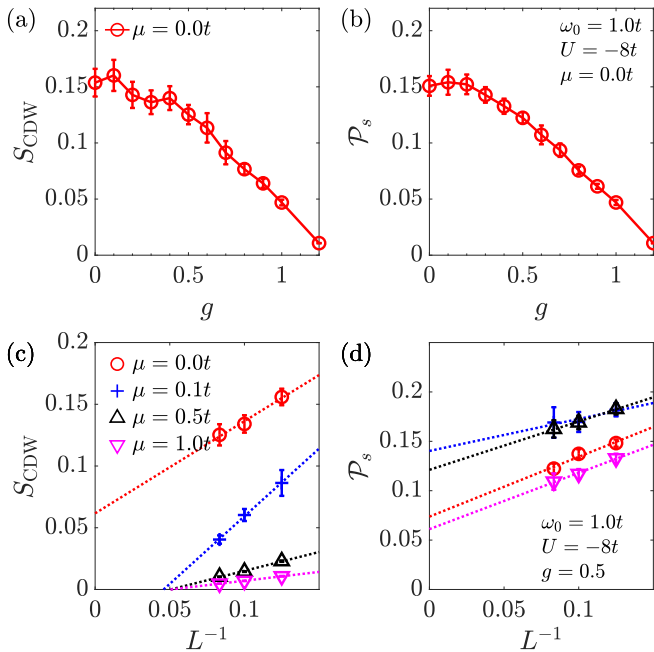
FIG. 4. (a) CDW structure factor S_{CDW} and (b) s-wave pairing correlation $\mathcal{P}_s$ against electron-phonon coupling g at half-filling. (c) Finite-size scaling of S_{CDW} and (d) $\mathcal{P}_s$ at $g = 0.5$. For all subplots, phonon frequency $\omega_0 = 1.0t$ and electron-electron coupling $U = -8t$.

At $g = 0.0$, the system is described purely by the attractive Hubbard model. The degenerate CDW/pairing symmetry is lifted immediately with finite μ: Away from half-filling, S_{CDW} falls rapidly [Fig. 3(b)] while $\mathcal{P}_s$ is maximized at an intermediate density [Fig. 3(c)]. At $g = 0.5$, we observe a decrease in both S_{CDW} [Fig. 3(b)] and $\mathcal{P}_s$ [Fig. 3(c)]. The effect of g on the half-filled attractive Hubbard model is further studied in Figs. 4(a) and 4(b). As g increases, both S_{CDW} and $\mathcal{P}_s$, which are known to be equal at half-filling, decrease. This suggests that the SSH electron-phonon interaction works against the attractive Hubbard interaction at and away from half-filling. While the attractive Hubbard U and SSH g support different ground state phases, we find no evidence of an intermediate phase for the parameters we have studied. At $g = 1.2$, the strong SSH electron-phonon interaction dominates and the half-filled ground state becomes the gapped $q = (\pi, \pi)$ BOW.

In Figs. 4(c) and 4(d), we show the finite-size scaling of S_{CDW} and $\mathcal{P}_s$ at $g = 0.5$. As the pure attractive Hubbard model, S_{CDW} extrapolates to a finite value only at half-filling $\mu = 0$. In Fig. 4(c), an infinitesimal $|\mu| = 0.1$ is enough to destroy the CDW phase. In Fig. 4(d), $\mathcal{P}_s$ extrapolates to a finite value for a large range of μ. These finite-size scaling results show that the electron-phonon coupling g does not

qualitatively change the attractive Hubbard ground state for $g < g_c$. At half-filling, the ground state is either the SSH BOW or the degenerate attractive Hubbard CDW/s-wave pairing phase. Away from half-filling, the ground state always exhibits s-wave pairing, albeit moderated by the magnitude of the electron-phonon coupling g.

Conclusions. In this Letter, we present a DQMC study of the single-orbital square lattice attractive SSHH model. Because of the lack of a sign problem, we can study the interplay between the (SSH) electron-phonon interaction and electron-electron interactions in the ground state.

At half-filling, we find a first-order quantum phase transition between the BOW phase and the degenerate CDW/s-wave pairing phase. At higher g, the ground state remains in the degenerate CDW/s-wave pairing phase until the BOW sets in for large enough g. Away from half-filling, the CDW phase and BOW phase are both unstable. The ground state is s-wave pairing but the order parameter can be reduced by larger electron-phonon interactions. In addition, we show the effects of phonon frequency. As it decreases, phonon fluctuations increase and the electron-phonon mechanism becomes more robust. As in the case of the Holstein model, this leads to a reduction in s-wave pairing. Other than pointing out that its magnitude becomes much smaller at lower phonon frequencies, we cannot rule out the possibility of its existence.

The fundamental feature of the SSH Hamiltonian is the modulation of the intersite hopping by a phonon displacement X_{ij}. A related model in which this electron-phonon interaction and on-site U is present has been suggested as a description of the Kondo effect arising from a vibrating magnetic ion [78–85]. Recent advancements in experimental setups have opened up the possibility to study different variants of the SSH model physically [86–90]. These studies have focused on the topological properties of the static SSH model, which assumes a frozen phonon structure. Our theoretical work expands further by studying the SSH model with full phonon dynamics. Moving forward, it will be interesting to investigate further the low U regime, which even in the absence of electron-phonon coupling is much harder to study [91–93]. Another area that could benefit from further investigation is the regime of low phonon frequencies which, due to smaller gaps, require larger systems and lower temperatures.

[1] J. Hubbard, Electron correlations in narrow energy bands, Proc. R. Soc. London, Ser. A **276**, 238 (1963).

[2] M. C. Gutzwiller, Effect of correlation on the ferromagnetism of transition metals, Phys. Rev. Lett. **10**, 159 (1963).

[3] J. Kanamori, Electron correlation and ferromagnetism of transition metals, Prog. Theor. Phys. **30**, 275 (1963).

[4] J. Hubbard, Electron correlations in narrow energy bands. II. The degenerate band case, Proc. R. Soc. London, Ser. A **277**, 237 (1964).

[5] J. Hubbard, Electron correlations in narrow energy bands. III. An improved solution, Proc. R. Soc. London, Ser. A **281**, 401 (1964).

[6] H. Tasaki, The Hubbard model—an introduction and selected rigorous results, J. Phys.: Condens. Matter **10**, 4353 (1998).

[7] A. Georges, G. Kotliar, W. Krauth, and M. Rozenberg, Dynamical mean-field theory of strongly correlated fermion systems and the limit of infinite dimensions, Rev. Mod. Phys. **68**, 13 (1996).

[8] P. A. Lee, N. Nagaosa, and X.-G. Wen, Doping a Mott insulator: Physics of high-temperature superconductivity, Rev. Mod. Phys. **78**, 17 (2006).

[9] M. Qin, T. Schäfer, S. Andergassen, P. Corboz, and E. Gull, The Hubbard model: A computational perspective, Annu. Rev. Condens. Matter Phys. **13**, 275 (2022).

[10] D. P. Arovas, E. Berg, S. A. Kivelson, and S. Raghu, The Hubbard model, Annu. Rev. Condens. Matter Phys. **13**, 239 (2022).

[11] T. Holstein, Studies of polaron motion: Part I. The molecular-crystal model, Ann. Phys. **8**, 325 (1959).

[12] W. P. Su, J. R. Schrieffer, and A. J. Heeger, Solitons in polyacetylene, Phys. Rev. Lett. **42**, 1698 (1979).

[13] R. M. Noack, D. J. Scalapino, and R. T. Scalettar, Charge-density-wave and pairing susceptibilities in a two-dimensional electron-phonon model, Phys. Rev. Lett. **66**, 778 (1991).

[14] M. Vekić, R. M. Noack, and S. R. White, Charge-density waves versus superconductivity in the Holstein model with next-nearest-neighbor hopping, Phys. Rev. B **46**, 271 (1992).

[15] Y.-X. Zhang, W.-T. Chiu, N. C. Costa, G. G. Batrouni, and R. T. Scalettar, Charge order in the Holstein model on a honeycomb lattice, Phys. Rev. Lett. **122**, 077602 (2019).

[16] C. Chen, X. Y. Xu, Z. Y. Meng, and M. Hohenadler, Charge-density-wave transitions of Dirac fermions coupled to phonons, Phys. Rev. Lett. **122**, 077601 (2019).

[17] C. Feng, H. Guo, and R. T. Scalettar, Charge density waves on a half-filled decorated honeycomb lattice, Phys. Rev. B **101**, 205103 (2020).

[18] M. Weber and M. Hohenadler, Two-dimensional Holstein-Hubbard model: Critical temperature, Ising universality, and bipolaron liquid, Phys. Rev. B **98**, 085405 (2018).

[19] B. Cohen-Stead, N. C. Costa, E. Khatami, and R. T. Scalettar, Effect of strain on charge density wave order in the Holstein model, Phys. Rev. B **100**, 045125 (2019).

[20] Z.-X. Li, M. L. Cohen, and D.-H. Lee, Enhancement of superconductivity by frustrating the charge order, Phys. Rev. B **100**, 245105 (2019).

[21] C. Feng and R. T. Scalettar, Interplay of flat electronic bands with Holstein phonons, Phys. Rev. B **102**, 235152 (2020).

[22] B. Nosarzewski, E. W. Huang, P. M. Dee, I. Esterlis, B. Moritz, S. A. Kivelson, S. Johnston, and T. P. Devereaux, Superconductivity, charge density waves, and bipolarons in the Holstein model, Phys. Rev. B **103**, 235156 (2021).

[23] B. Xiao, N. C. Costa, E. Khatami, G. G. Batrouni, and R. T. Scalettar, Charge density wave and superconductivity in the disordered Holstein model, Phys. Rev. B **103**, L060501 (2021).

[24] O. Bradley, G. G. Batrouni, and R. T. Scalettar, Superconductivity and charge density wave order in the two-dimensional Holstein model, Phys. Rev. B **103**, 235104 (2021).

[25] P. M. Dee, J. Coulter, K. G. Kleiner, and S. Johnston, Relative importance of nonlinear electron-phonon coupling and vertex corrections in the Holstein model, Commun. Phys. **3**, 145 (2020).

[26] Y. Zhang, C. Feng, R. Mondaini, G. G. Batrouni, and R. T. Scalettar, Charge singlets and orbital-selective charge density wave transitions, Phys. Rev. B **106**, 115120 (2022).

[27] C. Kvande, C. Feng, F. Hébert, G. G. Batrouni, and R. T. Scalettar, Enhancement of charge density wave correlations in a Holstein model with an anharmonic phonon potential, Phys. Rev. B **108**, 075119 (2023).

[28] E. Fradkin and J. E. Hirsch, Phase diagram of one-dimensional electron-phonon systems. I. The Su-Schrieffer-Heeger model, Phys. Rev. B **27**, 1680 (1983).

[29] J. E. Hirsch and E. Fradkin, Phase diagram of one-dimensional electron-phonon systems. II. The molecular-crystal model, Phys. Rev. B **27**, 4302 (1983).

[30] H. Zheng, D. Feinberg, and M. Avignon, Effect of quantum fluctuations on the Peierls dimerization in the one-dimensional molecular-crystal model, Phys. Rev. B **39**, 9405 (1989).

[31] R. H. McKenzie, C. J. Hamer, and D. W. Murray, Quantum Monte Carlo study of the one-dimensional Holstein model of spinless fermions, Phys. Rev. B **53**, 9676 (1996).

[32] P. Sengupta, A. W. Sandvik, and D. K. Campbell, Peierls transition in the presence of finite-frequency phonons in the one-dimensional extended Peierls-Hubbard model at half-filling, Phys. Rev. B **67**, 245103 (2003).

[33] W. Barford and R. J. Bursill, Effect of quantum lattice fluctuations on the Peierls broken-symmetry ground state, Phys. Rev. B **73**, 045106 (2006).

[34] C. J. Pearson, W. Barford, and R. J. Bursill, Quantized lattice dynamic effects on the Peierls transition of the extended Hubbard-Peierls model, Phys. Rev. B **83**, 195105 (2011).

[35] H. Bakrim and C. Bourbonnais, Nature of ground states in one-dimensional electron-phonon Hubbard models at half filling, Phys. Rev. B **91**, 085114 (2015).

[36] M. Weber, F. F. Assaad, and M. Hohenadler, Excitation spectra and correlation functions of quantum Su-Schrieffer-Heeger models, Phys. Rev. B **91**, 245147 (2015).

[37] M. Weber, F. Parisen Toldin, and M. Hohenadler, Competing orders and unconventional criticality in the Su-Schrieffer-Heeger model, Phys. Rev. Res. **2**, 023013 (2020).

[38] B. Xing, W.-T. Chiu, D. Poletti, R. T. Scalettar, and G. Batrouni, Quantum Monte Carlo simulations of the 2D Su-Schrieffer-Heeger model, Phys. Rev. Lett. **126**, 017601 (2021).

[39] X. Cai, Z.-X. Li, and H. Yao, Antiferromagnetism induced by bond Su-Schrieffer-Heeger electron-phonon coupling: A quantum Monte Carlo study, Phys. Rev. Lett. **127**, 247203 (2021).

[40] A. Götz, S. Beyl, M. Hohenadler, and F. F. Assaad, Valence-bond solid to antiferromagnet transition in the two-dimensional Su-Schrieffer-Heeger model by Langevin dynamics, Phys. Rev. B **105**, 085151 (2022).

[41] S. M. Costa, B. Cohen-Stead, A. T. Ly, J. Neuhaus, and S. Johnston, A comparative determinant quantum Monte Carlo study of the acoustic and optical variants of the Su-Schrieffer-Heeger model, arXiv:2307.10058.

[42] E. Berger, P. Valášek, and W. von der Linden, Two-dimensional Hubbard-Holstein model, Phys. Rev. B **52**, 4806 (1995).

[43] J. K. Freericks and M. Jarrell, Competition between electron-phonon attraction and weak Coulomb repulsion, Phys. Rev. Lett. **75**, 2570 (1995).

[44] C. Honerkamp, H. C. Fu, and D.-H. Lee, Phonons and *d*-wave pairing in the two-dimensional Hubbard model, Phys. Rev. B **75**, 014503 (2007).

[45] E. A. Nowadnick, S. Johnston, B. Moritz, R. T. Scalettar, and T. P. Devereaux, Competition between antiferromagnetic and charge-density-wave order in the half-filled Hubbard-Holstein model, Phys. Rev. Lett. **109**, 246404 (2012).

[46] D. Wang, W.-S. Wang, and Q.-H. Wang, Phonon enhancement of electronic order and negative isotope effect in the Hubbard-Holstein model on a square lattice, Phys. Rev. B **92**, 195102 (2015).

[47] S. Johnston, E. A. Nowadnick, Y. F. Kung, B. Moritz, R. T. Scalettar, and T. P. Devereaux, Determinant quantum Monte Carlo study of the two-dimensional single-band Hubbard-Holstein model, Phys. Rev. B **87**, 235133 (2013).

[48] T. Ohgoe and M. Imada, Competition among superconducting, antiferromagnetic, and charge orders with intervention by phase separation in the 2D Holstein-Hubbard model, Phys. Rev. Lett. **119**, 197001 (2017).

[49] S. Karakuzu, L. F. Tocchio, S. Sorella, and F. Becca, Superconductivity, charge-density waves, antiferromagnetism, and phase separation in the Hubbard-Holstein model, Phys. Rev. B **96**, 205145 (2017).

[50] Y. Wang, I. Esterlis, T. Shi, J. I. Cirac, and E. Demler, Zero-temperature phases of the two-dimensional Hubbard-Holstein model: A non-Gaussian exact diagonalization study, Phys. Rev. Res. **2**, 043258 (2020).

[51] E. Y. Loh, Jr., J. E. Gubernatis, R. T. Scalettar, S. R. White, D. J. Scalapino, and R. L. Sugar, Sign problem in the numerical simulation of many-electron systems, Phys. Rev. B **41**, 9301 (1990).

[52] J. Gubernatis and X. Zhang, Negative weights in quantum Monte Carlo simulations at finite-temperatures using the auxiliary field method, Int. J. Mod. Phys. C **05**, 599 (1994).

[53] M. Troyer and U.-J. Wiese, Computational complexity and fundamental limitations to fermionic quantum Monte Carlo simulations, Phys. Rev. Lett. **94**, 170201 (2005).

[54] R. Mondaini, S. Tarat, and R. T. Scalettar, Quantum critical points and the sign problem, Science **375**, 418 (2022).

[55] S. Tarat, B. Xiao, R. Mondaini, and R. T. Scalettar, Deconvolving the components of the sign problem, Phys. Rev. B **105**, 045107 (2022).

[56] S. Karakuzu, A. Tanjaroon Ly, P. Mai, J. Neuhaus, T. A. Maier, and S. Johnston, Stripe correlations in the two-dimensional Hubbard-Holstein model, Commun. Phys. **5**, 311 (2022).

[57] C. Feng, B. Xing, D. Poletti, R. Scalettar, and G. Batrouni, Phase diagram of the Su-Schrieffer-Heeger-Hubbard model on a square lattice, Phys. Rev. B **106**, L081114 (2022).

[58] X. Cai, Z.-X. Li, and H. Yao, Robustness of antiferromagnetism in the Su-Schrieffer-Heeger Hubbard model, Phys. Rev. B **106**, L081115 (2022).

[59] H.-X. Wang, Y.-F. Jiang, and H. Yao, Robust *d*-wave superconductivity from the Su-Schrieffer-Heeger-Hubbard model: Possible route to high-temperature superconductivity, arXiv:2211.09143.

[60] Q.-G. Yang, D. Wang, and Q.-H. Wang, Functional renormalization group study of the two-dimensional Su-Schrieffer-Heeger-Hubbard model, Phys. Rev. B **106**, 245136 (2022).

[61] J. E. Hirsch, Two-dimensional Hubbard model: Numerical simulation study, Phys. Rev. B **31**, 4403 (1985).

[62] R. T. Scalettar, E. Y. Loh, J. E. Gubernatis, A. Moreo, S. R. White, D. J. Scalapino, R. L. Sugar, and E. Dagotto, Phase diagram of the two-dimensional negative-*U* Hubbard model, Phys. Rev. Lett. **62**, 1407 (1989).

[63] A. F. Ho, M. A. Cazalilla, and T. Giamarchi, Quantum simulation of the Hubbard model: The attractive route, Phys. Rev. A **79**, 033620 (2009).

[64] C. F. Chan, M. Gall, N. Wurz, and M. Köhl, Pair correlations in the attractive Hubbard model, Phys. Rev. Res. **2**, 023210 (2020).

[65] R. Blankenbecler, D. J. Scalapino, and R. L. Sugar, Monte Carlo calculations of coupled boson-fermion systems. I, Phys. Rev. D **24**, 2278 (1981).

[66] R. T. Scalettar, N. E. Bickers, and D. J. Scalapino, Competition of pairing and Peierls–charge-density-wave correlations in a two-dimensional electron-phonon model, Phys. Rev. B **40**, 197 (1989).

[67] G. G. Batrouni and R. T. Scalettar, Langevin simulations of a long-range electron-phonon model, Phys. Rev. B **99**, 035114 (2019).

[68] J. Gubernatis, N. Kawashima, and P. Werner, *Quantum Monte Carlo Methods: Algorithms for Lattice Models* (Cambridge University Press, Cambridge, UK, 2016).

[69] R. L. Stratonovich, On a method of calculating quantum distribution functions, Sov. Phys. Dokl. **2**, 416 (1957).

[70] J. Negele and H. Orland, *Quantum Many-Particle Systems* (Basic Books, New York, 1988).

[71] P. Fulde, *Electron Correlations in Molecules and Solids* (Springer, Berlin, 1995).

[72] C. P. Enz, *A Course on Many-Body Theory Applied to Solid-State Physics* (World Scientific, Singapore, 1992).

[73] A. Fetter and J. Walecka, *Quantum Theory of Many-Particle Systems*, Dover Books on Physics (Dover, New York, 2003).

[74] S. R. White, D. J. Scalapino, R. L. Sugar, N. E. Bickers, and R. T. Scalettar, Attractive and repulsive pairing interaction vertices for the two-dimensional Hubbard model, Phys. Rev. B **39**, 839 (1989).

[75] Other electron-electron pairings, such as the *d*-wave pairing, are much lower than the *s*-wave pairing (not shown).

[76] M. Hohenadler and G. G. Batrouni, Dominant charge density wave correlations in the Holstein model on the half-filled square lattice, Phys. Rev. B **100**, 165114 (2019).

[77] J. M. Kosterlitz, The critical properties of the two-dimensional XY model, J. Phys. C: Solid State Phys. **7**, 1046 (1974).

[78] S. Yotsuhashi, M. Kojima, H. Kusuonse, and K. Miyake, New aspects of quasi-Kondo physics: Two-level Kondo and strongly coupled local electron-phonon systems, J. Phys. Soc. Jpn. **74**, 49 (2005).

[79] K. Hattori, Y. Hirayama, and K. Miyake, Local heavy quasiparticle in four-level Kondo model, J. Phys. Soc. Jpn. **74**, 3306 (2005).

[80] K. Mitsumoto and Y. Ōno, Phonon softening and double-well potential formation due to electron-phonon interaction in heavy-fermion systems, Physica C: Superconductivity **426-431**, 330 (2005).

[81] T. Hotta, Quasi-Kondo phenomenon due to the dynamical Jahn-Teller effect, Phys. Rev. Lett. **96**, 197201 (2006).

[82] T. Hotta, Effect of rattling phonons on Sommerfeld constant, J. Phys. Soc. Jpn. **77**, 103711 (2008).

[83] T. Fuse and Y. Ōno, First order bipolaronic transition at finite temperature in the Holstein model, J. Phys. Soc. Jpn. **79**, 093702 (2010).

[84] K. Oshiba and K. Hotta, Electron mass enhancement due to anharmonic local phonons, J. Phys. Soc. Jpn. **80**, SA134 (2011).

[85] T. Fuse and T. Hotta, Effect of phonon-mediated attraction on the Kondo phenomenon emerging from a vibrating magnetic ion, JPS Conf. Proc. **3**, 016024 (2014).

[86] E. J. Meier, F. A. An, and B. Gadway, Observation of the topological soliton state in the Su-Schrieffer-Heeger model, Nat. Commun. **7**, 13986 (2016).

[87] M. Leder, C. Grossert, L. Sitta, M. Genske, A. Rosch, and M. Weitz, Real-space imaging of a topologically protected edge state with ultracold atoms in an amplitude-chirped optical lattice, Nat. Commun. **7**, 13112 (2016).

[88] S. Liu, W. Gao, Q. Zhang, S. Ma, L. Zhang, C. Liu, Y. J. Xiang, T. J. Cui, and S. Zhang, Topologically protected edge state in two-dimensional Su-Schrieffer-Heeger circuit, Research **2019**, 8609875 (2019).

[89] L.-Y. Zheng, V. Achilleos, O. Richoux, G. Theocharis, and V. Pagneux, Observation of edge waves in a two-dimensional Su-Schrieffer-Heeger acoustic network, Phys. Rev. Appl. **12**, 034014 (2019).

[90] J.-H. Chen, Z.-Z. Yang, W.-J. Yang, A.-Y. Guan, X.-Y. Zou, and J.-C. Cheng, Experimental realization of boundary-obstructed topological insulators using acoustic two-dimensional Su-Schrieffer-Heeger network, Appl. Phys. Lett. **120**, 253508 (2022).

[91] S. R. White, D. J. Scalapino, R. L. Sugar, E. Y. Loh, J. E. Gubernatis, and R. T. Scalettar, Numerical study of the two-dimensional Hubbard model, Phys. Rev. B **40**, 506 (1989).

[92] T. Pruschke and R. Zitzler, From Slater to Mott–Heisenberg physics: The antiferromagnetic phase of the Hubbard model, J. Phys.: Condens. Matter **15**, 7867 (2003).

[93] M. Raczkowski, F. F. Assaad, and M. Imada, Local moments versus itinerant antiferromagnetism: Magnetic phase diagram and spectral properties of the anisotropic square lattice Hubbard model, Phys. Rev. B **103**, 125137 (2021).

[94] https://www.nscc.sg.